Natural Resources for Human Health

visaga publishing house

Original Research

View Article online

Check for updates

Received 15 February 2025
Revised 14 April 2025
Accepted 12 May 2025
Available Online 12 June 2025

Edited by Kannan RR Rengasamy

KEYWORDS:
Bioactivity
Drug discovery
In silico
Natural resources
Neuroprotective agent
Protein-protein interaction

Natr Resour Human Health 2025; 5 (3): 376–392
https://doi.org/10.53365/nrfhh/204979
eISSN: 2583-1194
Copyright © 2025 Visagaa Publishing House

The supplementary information associated with this article available at: https://doi.org/10.53365/nrfhh/204979

Network Analysis of Neuroprotective Receptors and Molecular Docking Insights into *Amaranthus*-Derived Compounds

Mega Sonia Pertiwi[1], Irmanida Batubara[1,2,*], Rizka Fatriani[3], Setyanto Tri Wahyudi[2,4], Wisnu Ananta Kusuma[5,2], Trivadila Trivadila[1,2], Bambang Pontjo Priosoeryanto[6,2]

[1]Department of Chemistry, Faculty of Mathematics and Natural Sciences, IPB University, IPB Dramaga Campus, Bogor, West Java 16680, Indonesia
[2]Tropical Biopharmaca Research Center, International Research Institute of Food, Nutrition and Health, IPB University, Bogor, West Java, 16128, Indonesia
[3]Biology Study Program, Faculty of Science, Sumatera Institute of Technology, Lampung, Indonesia
[4]Departement of Physics, Faculty of Mathematics and Natural Sciences, IPB University, IPB Dramaga Campus, Bogor, West Java 16680, Indonesia
[5]Department of Computer Science, Faculty of Mathematics and Natural Sciences, IPB University, IPB Dramaga Campus, Bogor, West Java 16680, Indonesia
[6]School of Veterinary Medicine & Biomedical Sciences, IPB Dramaga Campus, Bogor, West Java 16680, Indonesia

ABSTRACT: Neurodegenerative diseases are marked by the progressive loss of specific neurons, leading to cognitive and motor impairments. This neurodegeneration occurs gradually and silently over the years, with continuous neuronal cell death before clinical symptoms emerge. Neuroprotection, which seeks to prevent or minimize neuronal damage, has gained increasing attention—particularly through natural compounds—as potential therapeutic agents. *Amaranthus* has demonstrated antioxidant, neuroprotective, and antidepressant properties; however, further biochemical investigations are required. This study integrates protein–protein interaction network (PPIN) analysis, molecular docking-based virtual screening, and molecular dynamics to identify key neuroprotective targets and bioactive compounds in *Amaranthus*. PPIN analysis of 27 neuroprotection-related proteins identified key hub proteins, including Dopamine D2 receptor (D2), metabotropic glutamate receptor 2 (mGlu2), 5-hydroxytryptamine receptor 1A (5HT1A), γ-aminobutyric acid B receptor (GABAb), metabotropic glutamate receptor 3 (mGlu3), SERT (serotonin reuptake transporter), cannabinoid type 1 receptor (CB1), Milestones of Recovery Scales (MORs), and monoamine oxidase B (MAOB) that play critical roles in neuronal survival and neurotransmission. Molecular docking-based virtual screening identified 10 ligands targeting MAOB, mGlu2, mGlu3, and GABAb receptors exhibiting lower binding energies than control ligands, suggesting strong interactions. Among these, dihydrokaempferol showed the most favorable profile, combining high binding affinity, strong predicted bioactivity, and interaction stability in molecular dynamics simulations,

* Corresponding author.
E-mail address: ime@apps.ipb.ac.id (Irmanida Batubara)

This is an open access article under the CC BY-NC-ND license (http://creativecommons.org/licenses/by-nc-nd/4.0/).

despite some pharmacokinetic limitations" might better reflect the nature of the findings. These findings highlight the therapeutic potential of *Amaranthus*-derived compounds for neurodegenerative diseases.

1. INTRODUCTION

Neurodegenerative diseases are pathological conditions characterized by the selective damage or loss of specific groups of neurons. This neuronal loss disrupts the normal functioning of the central nervous system (CNS), impairing cognitive, motor, or both functions. The neurodegeneration process occurs silently over the years, with continuous nerve cell death throughout life before the first clinical symptoms appear (Silva and Pogačnik, 2020). Understanding the mechanisms underlying these changes has emerged as one of the most significant neurobiological challenges in recent decades, driving efforts to develop strategies to slow cognitive aging and preserve brain health (González-Fuentes et al., 2018).

In response to these challenges, the field of neuroprotection has gained prominence that encompasses strategies and mechanisms aimed at shielding the CNS from neuronal damage and preserving its functional integrity (Pertiwi et al., 2024). Key neuroprotective strategies often target oxidative stress and excitotoxicity, two critical contributors to neuronal cell death and neurodegeneration. Therapeutic interventions, including the use of glutamate antagonists and antioxidants, have demonstrated efficacy in both research and clinical settings (Lalkovičová and Danielisová, 2016).

Recent studies highlight the significant potential of natural resources in neuroprotection. Anjum et al. (2024) demonstrated that ethanolic extract of *Mentha piperita* significantly improved motor function, enhanced antioxidant capacity, and reduced neurodegeneration in the substantia nigra, highlighting its antioxidant and neuroprotective properties. Beppe et al. (2024) reported that an aqueous extract of *Ximenia americana* attenuated cognitive impairment induced by diazepam, further suggesting its neuroprotective and antioxidant effects. Malik et al. (2024) found that *Acorus calamus* effectively restored the antioxidant state of the brain and provided neuroprotection by reducing scopolamine-induced oxidative damage.

Similarly, *Amaranthus* has attracted considerable scientific interest for its many health benefits. Traditionally, it was used as a sedative, and modern research highlights the antioxidant, neuroprotective, and antidepressant properties of its leaves. These therapeutic effects affect critical brain functions, including sensory processing, movement regulation, mental and emotional balance, cognitive performance, and social behavior (Pertiwi et al., 2024). Despite its promising potential, further biochemical studies are required to validate and expand the understanding of these properties.

Protein-protein interactions (PPI) are vital to biological processes and the PPI network (PPIN) analysis reveals interaction principles and functional patterns in the cellular systems, enhancing our understanding of the biological system, also facilitating insights into disease mechanisms, gene and protein perturbations, and potential drug targets (Yugandhar and Gomiha, 2016). Grewal et al. (2024) used PPIN analysis to identify amyloid precursor protein as a potential hub protein and a key contributor to Alzheimer disease pathogenesis. Robati et al. (2024) used PPIN analysis to identify key proteins and genes involved in the cellular aging process and investigate the relationship between proteins in cellular rutin metabolic cycles.

Molecular docking plays a central role in drug discovery by providing detailed insights into molecular interactions that underpin key biological processes. It facilitates the identification and development of potential therapeutic agents (Shamsi et al., 2024). As a cost-effective and efficient alternative to experimental high-throughput screening, virtual screening allows compounds from digital libraries to be docked individually against target proteins, prioritizing candidates with the most favorable predicted binding affinities for further validation. Notably, virtual libraries often include unsynthesized compounds, enabling access to inexpensive and readily available molecules, thereby reducing both costs and dependency on docking precision (Paggi et al., 2024).

While docking provides a static approximation of binding interactions, its accuracy can be significantly enhanced through molecular dynamics (MD) simulations that model the real-time motion of all atoms within a system. This enables a more realistic prediction of binding poses and energetics (Paggi et al., 2024). At a quantitative level, MD-based approaches—particularly those employing free energy calculations—offer superior accuracy in estimating ligand binding affinities compared to docking alone (Hollingsworth and Dror, 2018).

The neuroprotective potential of *Amaranthus* has been previously reported, yet the specific bioactive compounds and their molecular targets remain largely unexplored. The aim

of this study was to identify key protein targets involved in neuroprotection through the PPIN analysis and to evaluate neuroprotective potential of *Amaranthus*-derived compounds via molecular docking and dynamics.

2. MATERIALS AND METHODS

2.1. Protein ID mapping

Protein identifier (ID) mapping was performed using the UniProt database (Consortium, 2023), with Protein Data Bank (PDB) ID and protein names as input. A total of 32 proteins (Table 1) were selected for further analysis based on a targeted literature review and database screening. The inclusion criteria were: (1) relevance to neuroprotective mechanisms or neuropsychiatric disorders (e.g., major depressive disorder, anxiety, and mood disorders) and (2) availability of 3D (three-dimensional) structures or interaction data in UniProt and PDB.

2.2. Protein-protein interaction

The proteins obtained from the ID mapping process were de-duplicated. The resulting list was input into the STRING (search tool for the retrieval of interacting genes/proteins) database (https://string-db.org/) (Szklarczyk et al., 2022) to identify interactions among the proteins. The analysis was performed using the following parameters: organism (*Homo sapiens*), network type (full STRING network), and minimum required interaction score (medium confidence threshold of 0.400).

2.3. Network analysis

The Cytoscape application was used to analyze the protein interaction network (Shannon et al., 2003). Centrality analyses performed included Betweenness Centrality, Degree, and Closeness Centrality. The CytoHubba plugin was employed to identify key proteins (hub proteins). The centrality measure used was Maximal Clique Centrality (MCC), defined by Equation 1.

$$MCC(v) = \sum_{C \in S(v)} (|C| - 1)! \qquad \text{Equation 1}$$

Where S(v) is the collection of maximal cliques containing v; (|C| – 1)! is the product of all positive integers less than |C|; and if there is no edge between the neighbors of node v, then MCC(v) is equal to its degree (Chin et al., 2014).

2.4. Molecular docking

The molecular docking method described by Cahya et al. (2024) was used with some modifications.

2.4.1. Ligand preparation

The ligand preparation process involved in the retrieval of 240 *Amaranthus*-derived compounds is hereafter referred to as test ligands (listed in Table S1, Supplementary). These compounds were selected based on literature reports of the liquid chromatography-mass spectrometry (LC-MS) phytochemical profiling of four commonly studied *Amaranthus* species: *A. viridis, A. spinosus, A. tricolor*, and *A. caudatus*. The keyword search was conducted using combinations of these species such as "LC-MS *Amaranthus viridis*"; "LC-MS *Amaranthus spinosus*"; "LC-MS *Amaranthus tricolor*"; and "LC-MS *Amaranthus caudatus*" in Google Scholar. LC-MS-based identification was used to ensure that only experimentally detected and naturally occurring compounds were considered, and then the compounds with the available 3D structural data in the PubChem database (https://pubchem.ncbi.nlm.nih.gov/) were used. The 3D structures were downloaded in .sdf format and converted to .pdb format using Open Babel software. Ligand optimization was then performed using AutoDock Tools v1.5.6, which included hydrogen atoms, calculation of Gasteiger charges, merging of nonpolar hydrogens, and the definition of rotatable bonds. Finally, the ligands were saved as .pdbqt format for docking analysis.

2.4.2. Receptor preparation

The receptors used in this study were key receptors selected on the basis of MCC value. The receptors were obtained in .pdb format from the PDB website (www.rscb.org/pdb). The preparation of these receptors involved separation of natural ligands, removal of water molecules, and elimination of attached residues using PyMOL software. The receptors were further optimized using AutoDock Tools version 1.5.6 by adding hydrogen atoms, calculating Gasteiger charges, and regulating the fusion of nonpolar hydrogens. The optimized receptors were saved in .pdbqt format for further analysis.

2.4.3. Redocking and blind docking

The receptor preparation process involved separating natural ligands, followed by redocking experiments with their respective receptors using AutoDock Vina 1.1.2. Molecular docking validation was performed using grid box sizes spaced at 1.000 Å intervals centered on the coordinates of the corresponding natural ligands. This process was repeated three times, and the grid box size that yielded the lowest Root Mean Square Deviation (RMSD) value was selected for further molecular docking analyses. Meanwhile, blind docking was performed

Table 1
List of 32 proteins associated with neuroprotection and mental health.

Number	Protein	Gene	Physiological Relevance	PDB ID	Reference
1	Nrf2-Keap1	KEAP1 INRF2 KIAA0132 KLHL19	Anxiety, prevent depression, antidepression, bipolar	8XGV	(Hashimoto, 2018)
2	P2X7R	P2RX7	MDD, anxiety	5XW6	(Jaronczyk and Walory, 2022; Qi et al., 2024)
3	5-HT1A	GNAI1	MDD	7E2Y/8PKM	(Ostrowska et al., 2018)
4	D3	DRD3	MDD	3PBL	(Elek et al., 2021)
5	D2	DRD2	MDD	6CM4	(Elek et al., 2021)
6	MORs	OPRM1 MOR1	Dysregulating this receptor may cause depression	7UL4/4DKL/ 5C1M	(Jaronczyk and Walory, 2022; Jelen et al., 2022)
7	KORs	Not found	Dysregulating this receptor may cause depression	Not found	(Jaronczyk and Walory, 2022; Jelen et al., 2022)
8	DORs	Not found	Dysregulating this receptor may cause depression	Not found	(Jaronczyk and Walory, 2022; Jelen et al., 2022)
9	NOP	Not found	Dysregulating this receptor may cause depression	Not found	(Jaronczyk and Walory, 2022; Jelen et al., 2022)
10	mGlu2	GRM2 GPRC1B MGLUR2	MDD, Mood disorder	5CNI	(Jaronczyk and Walory, 2022)
11	mGlu3	GRM3 GPRC1C MGLUR3	MDD, Mood disorder	5CNK	(Jaronczyk and Walory, 2022)
12	GPR26	GPR26	MDD	Not found	(Albert, 2020; Jaronczyk and Walory, 2022)
13	GPR56	ADGRG1 GPR56 TM7LN4 TM7XN1 UNQ540/PRO1083	MDD	7SF8	(Albert, 2020; Jaronczyk and Walory, 2022)
14	GPR52	GPR52	MDD	6LI2	(Albert, 2020; Jaronczyk and Walory, 2022)
15	GPR158	GPR158 KIAA1136	MDD	7SHE	(Albert, 2020; Jaronczyk and Walory, 2022)
16	TAAR1	TAAR1 TA1 TAR1 TRAR1	MDD	8W8A	(Jaronczyk and Walory, 2022)
17	TAAR5	TAAR5 PNR	MDD	Not found	(Jaronczyk and Walory, 2022)
18	CB1	CNR1 CNR	MDD	5TGZ/ 5XRA	(Jaronczyk and Walory, 2022; Patel and Hillard, 2009)
19	CB2	CNR2 CB2A CB2B	MDD	2HFF	(Jaronczyk and Walory, 2022; Patel and Hillard, 2009)
20	M1	CHRM1	MDD	6ZFZ	(Jaronczyk and Walory, 2022)
21	M2	CHRM2	MDD	5ZKC	(Jaronczyk and Walory, 2022)
22	GABAb	GABBR2 GPR51 GPRC3B	MDD	4MR7	(Jaronczyk and Walory, 2022)
23	GABAb	GABBR1 GPRC3A	MDD	4MR7	(Jaronczyk and Walory, 2022)
24	NK1	TACR1 NK1R TAC1R	MDD	6HLP	(Jaronczyk and Walory, 2022)
25	CCK2	CCKBR CCKRB	MDD	7F8W	(Jaronczyk and Walory, 2022)
26	Leucine transporter	Not found	MDD	2A65	(Jaronczyk and Walory, 2022)
27	NET	SLC18A1 VAT1 VMAT1	MDD, ADHD	8TGL	(Jaronczyk and Walory, 2022)
28	SERT	SLC6A4 HTT SERT	MDD	5I6X	(Jaronczyk and Walory, 2022; Moazzem Hossen et al., 2021)
29	DAT	Not found	MDD	Not found	(Jaronczyk and Walory, 2022)
30	Mineralocorticoid receptor	NR3C2 MCR MLR	Sleep behavior, memory storage, and anxiety, MDD	2AA2	(Bledsoe et al., 2005; Jaronczyk and Walory, 2022)
31	MAOB	MAOB	Neurodegenerative disease	2XCG	(Lv et al., 2023)
32	Glycogen synthase kinase 3s	GSK3B	Neuroprotection	4PTE	(Rayasam et al., 2009)

using grid box sizes spaced at 1.000 Å intervals centered on the macromolecule coordinates. This process was also repeated three times and the conformation with the lowest binding energy was selected. The grid box size and center coordinates at 1.000 Å spacing intervals of the selected ligand conformation were stored for subsequent molecular docking analyses.

2.4.4. Virtual screening

Molecular docking simulations were conducted using AutoDock Vina 1.1.2 against their respective receptors. Docking parameters, including grid box dimensions, spacing, and coordinate points, were determined from both validation and blind docking results. The grid parameter used (center_x, center_y, and center_z, respectively) for each protein PDB ID were 50.742, 161.373, 30.939 (2XCG); –50.735, 22.457, –27.419 (4MR7); 2.026, 15.920, –58.785 (5C1M); 202.777, 46.765, 28.721 (5CNI); 21.588, –17.595, 51.595 (5CNK); –32.314, –21.112, 2.120 (5I6X); 48.771, 40.858, 299.565 (5TGZ); 15.668, 5.065, –17.580 (6CM4); and 108.981, 118.548, 95.060 (8PKM). The grid box size used for all protein were 20 × 20 × 20 with 1.000 Å spacing intervals. A configuration file detailing the grid box size and coordinates was created within the Vina directory. The docking process was then initiated from the Command Prompt (CMD). The output was generated as .pdbqt files, accompanied by a "log.txt" file containing the binding energy (ΔG) values. The ΔG values for the test ligands were compared with those of the cocrystal or control ligands to assess the spontaneity of ligand-receptor interactions. The top 10 test ligands with the most negative ΔG values were selected as the preferred ligands. The selected ligand was loaded in to the receptor using the PyMOL software and saved in the *pdb format. The file then opened using Discovery Studio Visualizer and LigPlot+ software to assess the binding site similarity (BSS) between the selected ligand and the cocrystal or control ligand.

2.5. Absorption, distribution, metabolism, excretion, and toxicology and bioactivity

Ligands with a BSS percentage greater than 50% were analyzed for their physicochemical properties, druglikeness, and medicinal chemistry using the SwissADME tool available at http://swissadme.ch/. The structures of the compound were uploaded in the SMILES (Simplified Molecular Input Line Entry System) code. The analysis was performed based on parameters consistent with Lipinski's Rules of Five, Ghose, Veber, Egan, Muegge, pan assay interference compounds (PAINS), and BRENK. Ligands that met all these parameters were used for further analysis. Absorption, distribution, metabolism, excretion, and toxicity (ADMET) predictions were performed using the pkCSM and admet-SAR websites. Meanwhile, bioactivity predictions were performed using the Way2Drug platform.

2.6. Molecular dynamics

The MD method was used as described on the website https://ambermd.org/tutorials/ and by Awaluddin et al. (2021) with some modifications.

2.6.1. Preparation of protein and ligand

MD simulations for the selected protein-ligand complexes were performed using the AMBER20 software package. Prior to simulation, the complexes were prepared with Pdb4amber, which involved the removal of water molecules and hydrogen atoms. The processed files were further refined for simulation using ambpdb and pdbamber scripts.

2.6.2. Relaxation

The relaxation step included minimization, heating, and equilibration, and simulation began with energy minimization focused on the added water and ions. Water molecules were placed using LEaP in positions optimized for water-water interactions, without considering solute or ion presence. During minimization, all other system components were restrained. Each minimization phase comprised 10,000 cycles, beginning with 500 steps using the Steepest Descent method, followed by the Conjugate Gradient algorithm for the remaining steps. Then, the system was gradually heated from 100 K to 298 K for over 1 ns (nanosecond) under constant volume. Initial random velocities followed a Maxwell-Boltzmann distribution. Following heating, the system was relaxed at constant pressure for 1 ns to allow the simulation box density to equilibrate. Then, positional restraints were reduced stepwise. An initial 1 ns run was performed with 10 kcal/mol·Å² restraints. Minimization was repeated with restraints applied only to the protein backbone. Successive 1 ns simulation at constant pressure were conducted with decreasing backbone restraints: first 10 kcal/mol·Å², then 1 kcal/mol·Å², and finally 0.1 kcal/mol·Å². The final relaxation step was carried out with no restraints for 1 ns at constant pressure. A small time step (1 fs [femtosecond]) was maintained, and center of mass motions were removed every 1000 steps to ensure system stability.

2.6.3. Production run

The next stage involved the production run using PMEMD. CUDA, aimed at observing the unrestrained, natural motion of molecules. This simulation is performed under an NPT ensemble (constant number of particles, pressure, and temperature)

for 200 ns at a fixed temperature. Post simulation analysis includes RMSD to assess system stability. The relative binding free energy was estimated using the Molecular Mechanics/Generalized Born Surface Area (MM/GBSA) method.

3. RESULTS

3.1. Protein ID mapping

The goal of protein ID mapping is to verify and standardize the protein identifiers of 32 selected proteins to ensure consistency and enable subsequent functional annotation and data integration. Based on the 32 selected proteins, 27 were verified using the Uniprot's IDmapping tool. The list is available in Supplementary Table S2.

3.2. Protein-protein interaction

The aim of the protein-protein interactions was to identify key hub proteins potentially involved in neuroprotective mechanisms. The PPIN generated by STRING analysis comprised 24 proteins and 57 interactions at a medium confidence level (0.400) encoded by the input gene set (Figure 1). Further analysis was performed using network analysis.

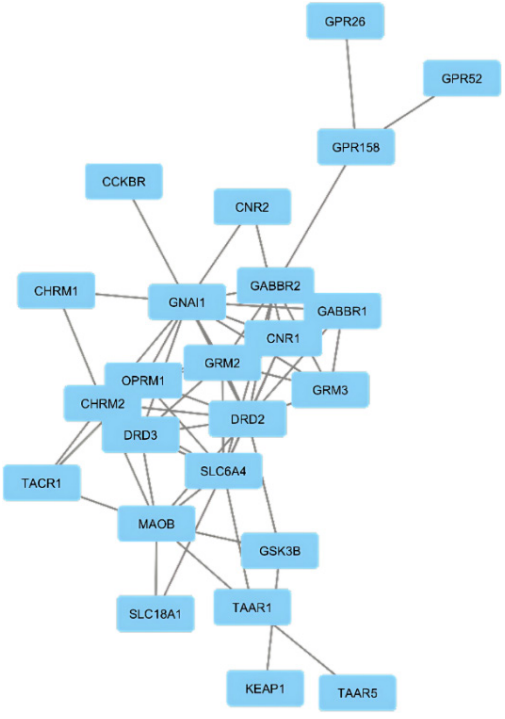

Figure 1. The network topology of protein-protein interactions (encoded by its gene) associated with neuroprotection and mental health

3.3. Network analysis

Centrality analysis of 24 proteins (Table 2) and MCC-ranked key proteins (Table 3, Figure 2) highlight the central role of the dopamine receptor D2 (DRD2) gene (D2). D2 shows the highest degree, centrality, and ranking scores, underscoring its key function in the dopaminergic system's link to neuroprotection. The guanine nucleotide-binding protein G[i] subunit alpha-1 (GNAI1) gene supports the importance of 5-hydroxytryptamine 1A receptor (5-HT1A), which shows high centrality through its connections across genes and pathways, emphasizing its role in neurotransmitter signaling as a G-protein subunit.

GABAb proteins, especially Gamma-aminobutyric acid type B receptor subunit 2 (GABBR2), exhibit high betweenness centrality, suggesting a bridging role in inhibitory neurotransmission; Gamma-aminobutyric acid type B receptor subunit 1 (GABBR1), ranked fifth by MCC, also plays a significant part. mGlu2 and mGlu3, encoded by glutamate metabotropic receptor 2 (GRM2) and glutamate

Table 2
Centrality analysis of 24 proteins.

Protein	Gene	Betweenness Centrality	Closeness Centrality	Degree
GABAb	GABBR2	0.2492	0.5476	7
5-HT1A	GNAI1	0.2233	0.5610	12
D2	DRD2	0.2018	0.6216	12
SERT	SLC6A4	0.1992	0.5750	10
GPR158	GPR158	0.1670	0.3833	3
MAOB	MAOB	0.1111	0.5111	8
Glycogen synthase kinase 3s	GSK3B	0.0870	0.4423	3
TAAR1	TAAR1	0.0870	0.4107	3
M2	CHRM2	0.0561	0.4894	6
mGlu2	GRM2	0.0369	0.5610	9
CB1	CNR1	0.0321	0.4894	6
MORs	OPRM1	0.0316	0.4894	6
D3	DRD3	0.0106	0.4792	5
NK1	TACR1	0.0023	0.3966	3
GABAb	GABBR1	0	0.4694	5
mGlu3	GRM3	0	0.4694	5
M1	CHRM1	0	0.4107	2
CB2	CNR2	0	0.3966	2
NET	SLC18A1	0	0.3966	2
CCK2	CCKBR	0	0.3651	1
GPR26	GPR26	0	0.2805	1
GPR52	GPR52	0	0.2805	1
Nrf2-Keap1	KEAP1	0	0.3108	1
TAAR5	TAAR5	0	0.2949	1

Table 3
Key proteins based on the MCC ranking system.

Rank	Protein	Gen	PDB ID	Score
1	D2	DRD2	6CM4	202
2	mGlu2	GRM2	5CNI	186
3	5HT1A	GNAI1	8PKM	157
4	GABAb	GABBR2	4RM7	127
5	mGlu3	GRM3	5CNK	120
5	GABAb	GABBR1	4MR7	120
6	SERT	SLC6A4	5I6X	52
7	CB1	CNR1	5TGZ	50
8	MORs	OPRM1	5C1M	49
9	MAOB	MAOB	2XCG	20

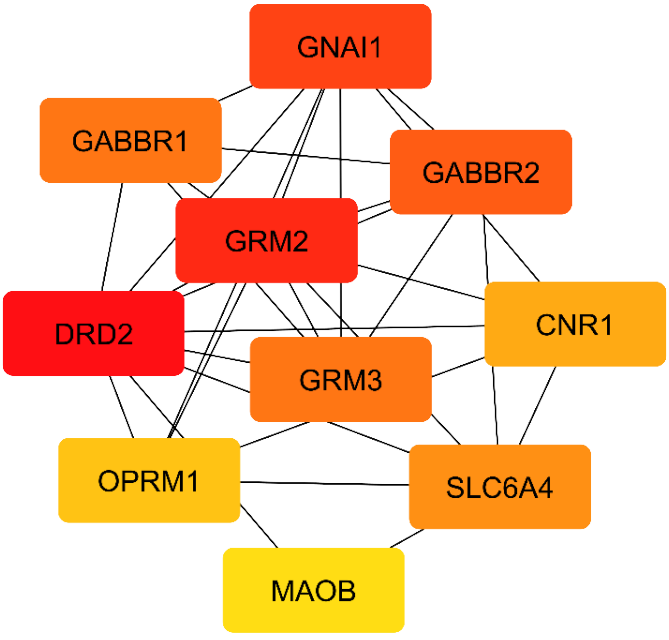

Figure 2. The network topology of the key proteins (encoded by its gene) based on the MCC ranking system, with colors indicating MCC scores: Red nodes show high MCC scores; yellow node shows low MCC scores.

metabotropic receptor 3 (GRM3), are key modulators of glutamate signaling. Among them, mGlu2 shows stronger connectivity and higher centrality, linking with major neuroprotective proteins (D2, GABAb, 5HT1A) and playing a central role in balancing excitatory and inhibitory transmission. Though mGlu3 is less connected, it remains important in glutamate regulation.

SERT (solute carrier family 6 member 4 [SLC64A]) holds a central position with high degree and closeness centrality, acting as a connector in neuroprotective pathways. CB1 (cannabinoid receptor 1 [CNR1]) and MORs (Mu-type opioid receptor [OPRM1]), while moderately connected, serve as key bridges in neuroprotective signaling. Last, MAOB shows moderate centrality, reflecting its role in monoamine metabolism. Together, these findings reveal a highly interconnected neuroprotective network, with D2, mGlu2, 5HT1A, GABAb, and mGlu3 as major regulatory hubs.

3.4. Molecular docking

Molecular docking was used to virtually screen *Amaranthus*-derived compounds for potential binding to target proteins. Redocking validated the docking protocol by reproducing known ligand binding modes, while blind docking identified potential unknown binding sites. Blind docking was performed instead of using cocrystallized ligands, as the available ligands did not match the desired pharmacological actions (e.g., agonist or antagonist). As shown in Table 4, all receptor-ligand complexes had RMSD values < 2 Å, confirming docking precision.

Binding affinities and BSS percentage values are summarized in Table S3 (Supplementary) and druglikeness and medicinal chemistry properties are summarized in Table S4 (Supplementary). Ligands with BSS percentage of > 50% and acceptable pharmacological profiles were shortlisted (Table 5). Several ligands showed better binding energy than control ligands (e.g., PDB: 2XCG, 5CNI, 5CNK, 4MR7), indicating potential for enhanced neuroprotective activity. Ligand-protein complexes (e.g., PDB: 4MR7, 5C1M, 5CNK, 5I6X, 5TGZ, 6CM4, 8PKM) were excluded due to violations of druglikeness or medicinal chemistry criteria (Table S4).

Figure 3 illustrates the binding interactions of selected ligands, showing whether they bind the same region as the

Table 4
RMSD and binding affinity value of redocking or blind docking.

Protein Receptor	PDB ID-Ligand Complex	RMSD (Å)	ΔG (kcal/mol)
5HT1A	8PKM-ZKV	0.25 ± 0.00	–12.20 ± 0.00
SERT	5I6X-8PR	0.40 ± 0.00	–13.00 ± 0.00
MORs	5C1M-BU72	0.45 ± 0.00	–12.70 ± 0.00
MAOB	2XCG-XCG	1.87 ± 0.00	–8.90 ± 0.00
D2	6CM4-Bromocriptine	n.d.	–10.73 ± 0.24
mGlu2	5CNI-LY354740	n.d.	–7.00 ± 0.08
mGlu3	5CNK-LY354740	n.d.	–6.87 ± 0.09
GABAb	4MR7-Baclofen	n.d.	–6.57 ± 0.12
CB1	5TGZ-WIN 55,212-2	n.d.	–9.20 ± 0.00

n.d.: not determined.

control ligand, suggesting comparable biological activity. Figure 4 presents the 3D interaction models of the selected ligands with the receptor, offering a structural perspective on their binding orientations. Table 6 details key amino acid interactions.

Notably, for MAOB, the control ligand binds mainly through hydrophobic interactions, forming hydrogen bonds with Tyr326 (tyrosine residue at position 326 in a protein) and Pro102. The selected ligand (e.g., apigenin), being more hydrophobic, shifts the interaction profile, possibly reducing polar contacts. However, its hydrogen bonding with Leu164, Thr201, and Glu84 suggests it may possess new polar groups, potentially enhancing MAOB inhibition and neuroprotective efficacy.

In mGlu2, residues Arg454 and Ala322 form hydrogen bonds with the control ligand but engage in hydrophobic interactions with kaempferol and hydrangenol, likely due to their aromatic structures. Dihydrokaempferol, in contrast, mirrors the control's hydrogen bonding but with shorter bond distances, suggesting better alignment and stronger binding, potentially enhancing its functional activity.

Table 5
Binding affinity of selected ligand with > 50% BSS and compliance of the druglikeness and medicinal chemistry.

Protein (PDB ID)	Ligand	ΔG (kcal/mol)	BSS %	Class
MAOB (2XCG)	Apigenin	–9.20 ± 0.00	90%	Flavonoid
mGlu2 (5CNI)	Kaempferol	–7.80 ± 0.00	75%	Flavonoid
	Dihydrokaempferol	–7.80 ± 0.00	87.5%	Flavonoid
	Hydrangenol	–7.80 ± 0.00	87.5%	Flavonoid

3.5. ADMET and bioactivity

To identify the most promising neuroprotective drug candidates, selected ligands were evaluated based on their physicochemical properties (Table 7), ADMET profiles (Table 8), and bioactivity (Table 9). These evaluations ensured that each ligand possessed favorable characteristics for biological activity, pharmacokinetics, and safety. Physicochemical analysis

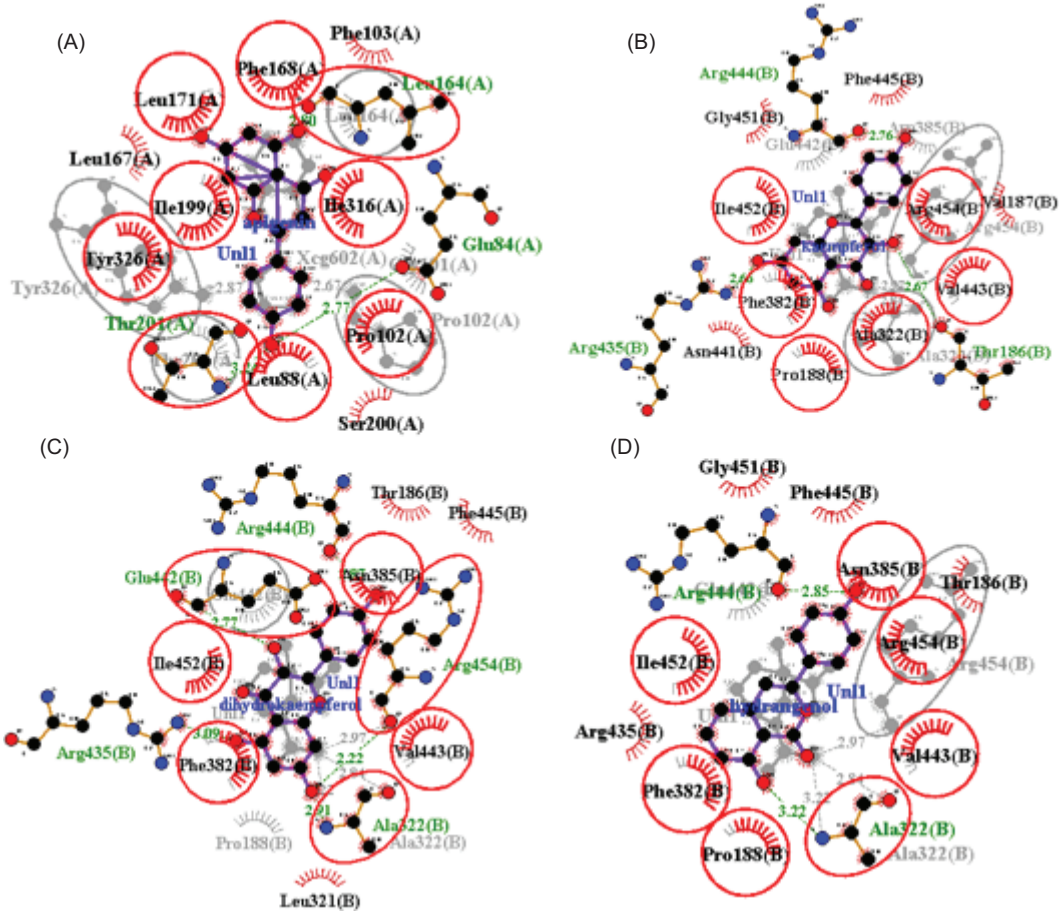

Figure 3. The similarity amino acid residue interaction between selected ligand and control ligand. (A) MAOB-apigenin; (B) mGlu2-kaempferol; (C) mGlu2-dihydrokaempferol; (D) mGlu2-hydrangenol.

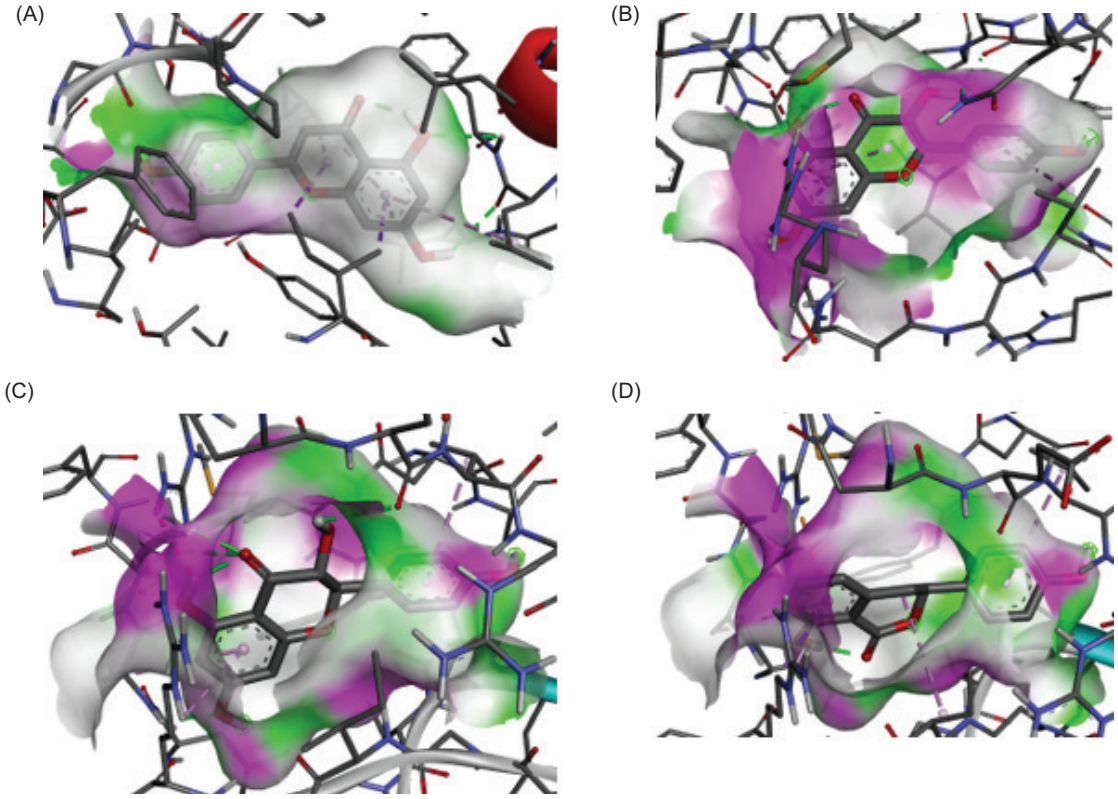

Figure 4. The visualization of 3D interaction between ligand and receptor. (A) MAOB-apigenin; (B) mGlu2-kaempferol; (C) mGlu2-dihydrokaempferol; (D) mGlu2-hydrangenol.

showed that all compounds complied with standard druglikeness criteria, including Lipinski's Rule of Five, Veber, Ghose, Egan, Muegge, PAINS, BRENK, and leadlikeness filters. The ligands exhibited total polar surface areas (TPSA) between 60 and 120 Å², optimal for absorption and permeability, and all maintained bioavailability scores above 0.50 with good solubility, indicating their potential as drug candidates.

ADMET evaluation revealed moderate water solubility (approximately –3 log mol/L) across all ligands. Most compounds demonstrated high intestinal permeability (log Papp > 0.9), with hydrangenol and apigenin showing absorption rates above 80% while kaempferol showed poor Caco-2 permeability. For CNS targeting, hydrangenol showed the highest blood-brain barrier (BBB) permeability, although apigenin exhibited superior CNS penetration, making it more suitable for neuroprotective applications. In the metabolism analysis, all ligands except dihydrokaempferol were predicted as CYP1A2 (cytochrome P450, family 1, subfamily A, polypeptide 2) inhibitors, suggesting a potential risk for drug-drug interactions. Excretion profiling showed moderate clearance values (log mL/min/kg between –1 and 1), and none of the compounds were substrates for the renal OCT2 (organic cation transporter 2), indicating minimal renal excretion involvement.

Toxicity predictions indicated no liver toxicity for any ligand. However, hydrangenol tested positive in the AMES test, suggesting potential genotoxicity and classified as extremely toxic in oral acute toxicity. Kaempferol and dihydrokaempferol were rated as highly toxic and apigenin had the lowest toxicity, indicating a relatively safer profile.

Bioactivity analysis showed that dihydrokaempferol had the strongest antioxidant and anti-inflammatory activities while hydrangenol scored the lowest in these categories. Kaempferol showed the highest antiapoptotic activity while hydrangenol demonstrated the strongest predicted activity in neurotransmitter antagonism and dopamine release. Apigenin showed potential in neurotransmitter uptake inhibition and was the top predicted MAOB inhibitor. Although dihydrokaempferol exhibited the weakest dopamine-related activity, it was the only compound predicted to have potential activity against neurodegenerative diseases. These findings highlight the importance of integrating multiple pharmacological and safety parameters to determine the most viable neuroprotective candidates.

Table 6
Amino acid residue interactions between the selected and control ligands.

Protein (PDB ID)	Ligand	Amino Acid Residues Interactions	
		H-Bond (Distance)	Hydrophobic
MAOB (2XCG)	XCG	Tyr326 (2.87 Å) Pro102 (2.67 Å)	Gly101 Ile316 Leu164 Phe168 Leu171 Ile199 Thr201 Leu88
	Apigenin	Leu164 (2.80 Å) Thr201 (3.24 Å) Glu84 (2.77 Å)	Phe168 Leu167 Phe103 Ile199 Ser200 Leu88 Pro102 Tyr326 Ile316 Leu171
mGlu2 (5CNI)	LY354740	Arg454 (2.97 Å) Ala322 (2.84 Å) Ala322 (3.22 Å)	Val443 Asn385 Pro188 Phe382 Ile452 Glu442
	Kaempferol	Arg435 (2.66 Å) Thr186 (2.67 Å) Arg444 (2.76 Å)	Val187 Gly451 Phe445 Val443 Asn441 Arg454 Ala322 Phe382 Ile452 Pro187
	Dihydrokaempferol	Ala322 (2.91 Å) Arg454 (2.22 Å) Arg435 (3.09 Å) Glu442 (2.77 Å) Arg444 (2.87 Å)	Thr186 Ile452 Phe382 Leu321 Val443 Asn385 Phe445
	Hydrangenol	Ala322 (3.22 Å) Arg444 (2.85 Å)	Gly451 Phe382 Thr186 Pro188 Ile452 Arg435 Arg454 Asn385 Val443 Phe445

Gly: Glycine; Ile: Isoleucine; Leu: Leucine; Phe: Phenylalanine; Thr: Threonine; Ser: Serine; Pro: Proline; Tyr: Tyrosine; Val: Valine; Asn: Asparagine; Arg: Arginine; Ala: Alanine; Glu: Glutamic Acid.

3.6. Molecular dynamics

MD helps confirm whether the ligand-protein interactions seen in docking are realistic, stable, and biologically meaningful under dynamic conditions, making it a critical step in validating potential neuroprotective drug candidates. The binding free energy are shown in Table 10, Figure 5, while RMSD and distance is shown in Figure 6 and Figure 7, respectively.

As shown in Table 10, all ligands exhibited negative van der Waals interaction energies (VDWAALS), indicating favorable steric interactions, with apigenin and dihydrokaempferol showing the most pronounced effects. Dihydrokaempferol also demonstrated the strongest electrostatic interaction energy (EEL), suggesting that charge-based interactions play a key role in stabilizing the complex. Dihydrokaempferol recorded the highest Generalized Born Solvation Energy (EGB), indicating reduced stability in aqueous environments compared to other ligands. In contrast, hydrangenol and kaempferol showed lower EGB values, reflecting more favorable polar solvation while apigenin exhibited moderate solvation energy. Nonpolar solvation energy (ESURF) was the most favorable for apigenin and dihydrokaempferol, suggesting better compatibility with nonpolar solvents.

Despite its gas-phase stability reflected by the most negative ΔG_{gas}, dihydrokaempferol exhibited the highest overall solvation energy (ΔG_{solv}), indicating lower solubility in water, whereas hydrangenol with the lowest ΔG_{solv} appeared to be the most readily solvated in aqueous conditions. All ligands displayed negative total binding free energies (ΔG_{total}), suggesting thermodynamically favorable interactions, with dihydrokaempferol showing the most favorable ΔG_{total}, followed by apigenin, identifying both as the most promising candidates in terms of binding affinity and complex stability. To further evaluate the stability of these interactions over time, binding energy fluctuations were monitored throughout the 200 ns simulation, as illustrated in Figure 5.

Based on Figure 5, dihydrokaempferol exhibited a lower average binding energy, approximately from –30 to –40 kcal/mol, with higher fluctuations observed between 75 ns and 150 ns. While dihydrokaempferol showed the lowest average binding energies, hydrangenol demonstrated the most consistent binding energy profile with minimal fluctuations over time. This indicates that hydrangenol forms a moderately strong yet highly stable complex with the receptor, suggesting it may be the most favorable ligand in terms of binding stability.

RMSD analysis of the protein, ligand, and the complex (Figure 6) aims to evaluate the dynamic stability of the protein-ligand complexes during the 200 ns MD simulation. The RMSD analysis highlights that hydrangenol formed the most

Table 7
Physicochemical properties of selected ligand

Ligand_Parameters_	MW (g/mol)	LogP	n-HA	n-HD	TPSA (Å^2)	Bioavailability Score
Kaempferol	286.24	1.58	6	4	111.13	0.55
Apigenin	270.24	2.11	5	3	90.90	0.55
Dihydrokampferol	288.25	1.02	6	4	107.22	0.55
Hydrangenol	256.25	2.40	4	2	66.76	0.55

MW: molecular weight; n-HA: number of hydrogen bond acceptor; n-HD: number of hydrogen bond donor; TPSA: topological polar surface area.

Table 8
ADMET values of selected ligand.

Parameter_ADMET value of Ligand	Kaempferol	Apigenin	Dihydrokaempferol	Hydrangenol
Absorption				
Water Solubility (log mol/L)	–3.04	–3.329	–2.967	–3.24
Caco-2 Permeability (log Papp 10^{-6} cm/s)	0.032	1.007	0.996	1.3
Human Intestinal Absorption (%Abs)	74.29	93.25	59.072	93.858
Distribution				
BBB Permeability (log BB)	–0.939	–0.734	–0.588	0.075
CNS Permeability (log PS)	–2.228	–2.061	–3.014	–2.136
Metabolism				
CYP2D6 substrate	N	N	N	N
CYP3A4 substrate	N	N	N	N
CYP1A2 inhibitor	Y	Y	N	Y
CYP2C9 inhibitor	N	N	N	N
CYP2D6 inhibitor	N	N	N	N
CYP3A4 inhibitor	N	N	N	N
Excretion				
Total Clearance (log mL/min/kg)	0.477	0.566	–0.003	0.485
Renal OCT2 substrate	N	N	N	N
Toxicity				
AMES Toxicity	N	N	N	Y
Hepatotoxicity	N	N	N	N
Acute Oral Toxicity	II	III	II	I

N: no; Y: yes; I: extremely toxic; II: highly toxic; III: moderately toxic.

Table 9
Bioactivity of selected ligands.

Parameter_Bioactivity of Ligand (Pa; Pi)	Kaempferol	Apigenin	Dihydrokaempferol	Hydrangenol
Antioxidant	0.856; 0.003	0.732; 0,004	0.946; 0.002	0.438; 0.009
Anti-inflammatory	0.676; 0.019	0.644; 0.024	0.722; 0.013	0.448; 0.073
Apoptotis Antagonist	0.309; 0.025	0.281; 0.042	0.195; 0.130	0.257; 0.061
Neurotransmitter Antagonist	0.599; 0.012	0.602; 0.012	0.622; 0.009	0.630; 0.008
Neurotransmitter Uptake Inhibitor	N/A	0.286; 0.229	N/A	N/A
MAOB Inhibitor	0.283; 0.004	0.412; 0.003	0.154; 0.010	0.147; 0.011
Dopamine Release Stimulant	0.217; 0.087	0.259; 0.053	0.164; 0.158	0.250; 0.060
Neurodegenerative Disease Treatment	N/A	N/A	0.228; 0.216	N/A

N/A: not available.

Table 10
Binding free energy using MM/GBSA analysis.

Ligand	VDWAALS	EEL	EGB	ESURF	ΔG_{gas}	ΔG_{solv}	ΔG_{total}
Apigenin	–35.309	–12.804	25.599	–5.161	–48.113	20.438	–27.675
Dihydrokaempferol	–34.716	–25.050	34.989	–5.026	–59.766	29.963	–29.803
Hydrangenol	–33.212	–10.741	23.012	–4.474	–43.953	18.538	–25.415
Kaempferol	–28.058	–9.349	21.916	–3.361	–37.407	18.555	–18.852

VDWAALS: Van der Waals interactions; EEL: Electrostatic Energy; EGB: Generalized Born Solvation Energy; ESURF: Nonpolar Solvation Energy; ΔG_{gas}: gas phase free energy; ΔG_{solv}: solvation free energy; ΔG_{total}: total binding free energy.

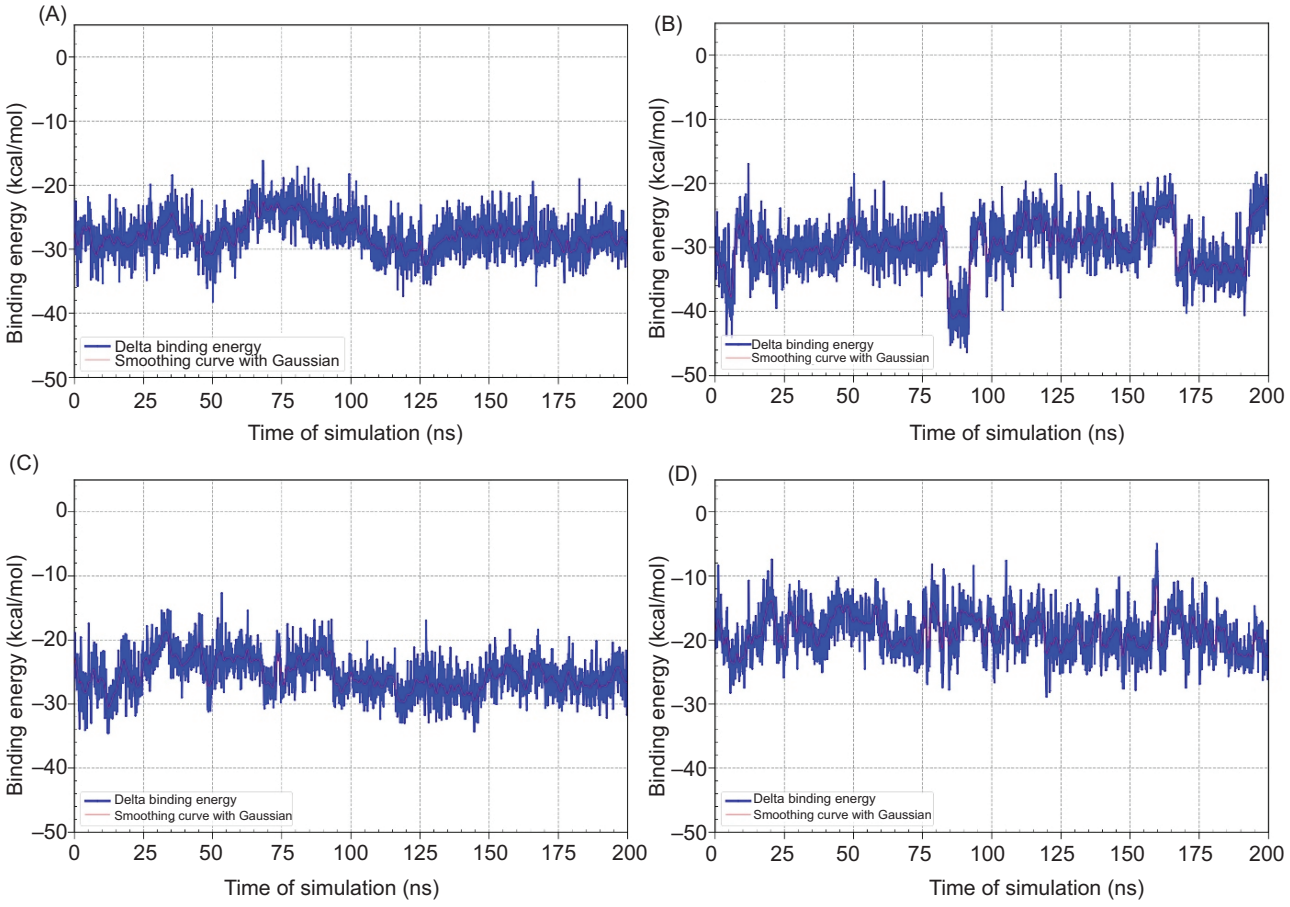

Figure 5. Time-dependent binding energy profiles of ligand-receptor complexes over 200 ns molecular dynamics simulations. (A) MAOB-apigenin; (B) mGlu2-kaempferol; (C) mGlu2-dihydrokaempferol; (D) mGlu2-hydrangenol.

stable protein-ligand complex, both in terms of protein structure and ligand retention. In contrast, dihydrokaempferol caused greater structural deviation in the complex despite maintaining its position within the binding site.

To further assess ligand stability within the binding pocket, distance analyses were performed over the 200 ns MD simulation (Figure 7). Distance analysis over 200 ns MD simulations revealed that dihydrokaempferol exhibited the most stable binding, with minimal pose deviation and consistent proximity to the binding site. Hydrangenol also maintained a stable interaction while kaempferol showed notable pose fluctuations, suggesting less stable binding. The protein-ligand distance remained steady across all complexes, although kaempferol displayed minor variation. Notably,

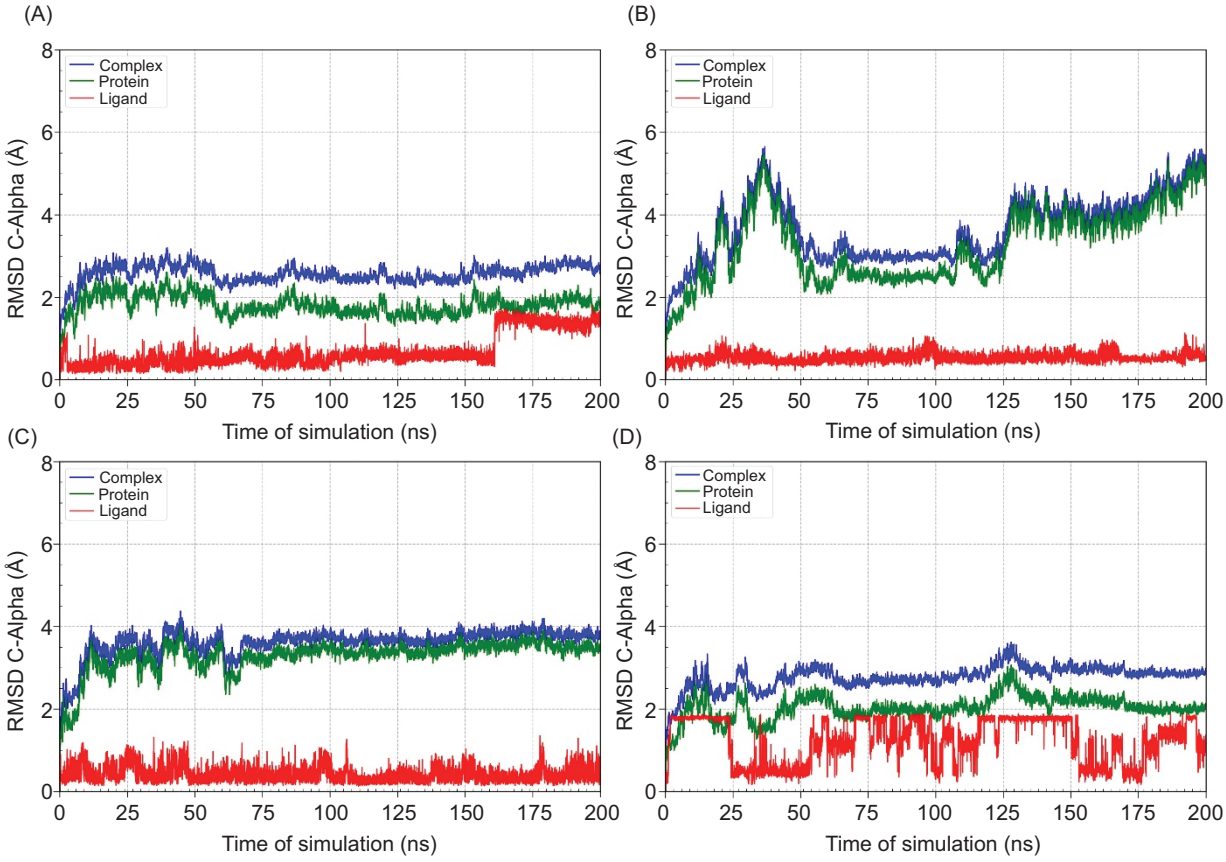

Figure 6. RMSD of C-Alpha atoms for the protein, ligand, and protein-ligand complex during 200 ns molecular dynamics simulations. (A) MAOB-apigenin; (B) mGlu2-kaempferol; (C) mGlu2-dihydrokaempferol; (D) mGlu2-hydrangenol.

apigenin exhibited slight fluctuations in the end to end distance, indicating potential system-level conformational changes.

4. DISCUSSIONS

Neurodegenerative diseases such as Alzheimer's and Parkinson's present a growing global health concern, yet effective treatments remain limited. As a result, natural products with neuroprotective properties—particularly compounds derived from *Amaranthus*—have gained attention for their antioxidant and anti-inflammatory potential (Kosmopoulou et al., 2024; Peter and Gandhi, 2017). Through the PPIN analysis, key neurodegeneration-related targets were identified, providing insights into how these bioactive compounds could modulate disease-associated pathways.

PPIN analysis of 27 neuroprotective-related proteins identified several hub targets, with D2 emerging as the most central protein, highlighting its essential role in dopaminergic transmission, synaptic plasticity, and neuronal survival (Sung et al., 2006; Zhou et al., 2022). 5HT1A also displayed high centrality, reflecting its involvement in neurotransmitter responses and its role in maintaining synaptic stability across cholinergic and GABAergic systems (Demos-Davies et al., 2024; Fang et al., 2021). Similarly, GABAb receptors—particularly GABBR2—were highlighted for their bridging role in neuroprotective signaling pathways, consistent with their known function in excitotoxicity suppression and neuronal regulation (Bi et al., 2020; Chen et al., 2019). Metabotropic glutamate receptors mGlu2 and mGlu3 were also identified as central to maintaining the balance of excitatory and inhibitory signaling (Srivastava et al., 2020).

Beyond these, the network analysis pointed to additional targets with neuroprotective relevance, including SERT, CB1, MORs, and MAOB. SERT regulates serotonin signaling that is critical for mood regulation and cognitive processes (Haase and Brown, 2015), while CB1 and MORs are known to modulate inflammation and β-amyloid toxicity, supporting neuronal integrity (Gargano et al., 2021; Wang et al., 2015). MAOB, although less central, plays a dual role in neurotransmitter metabolism and oxidative stress, and remains

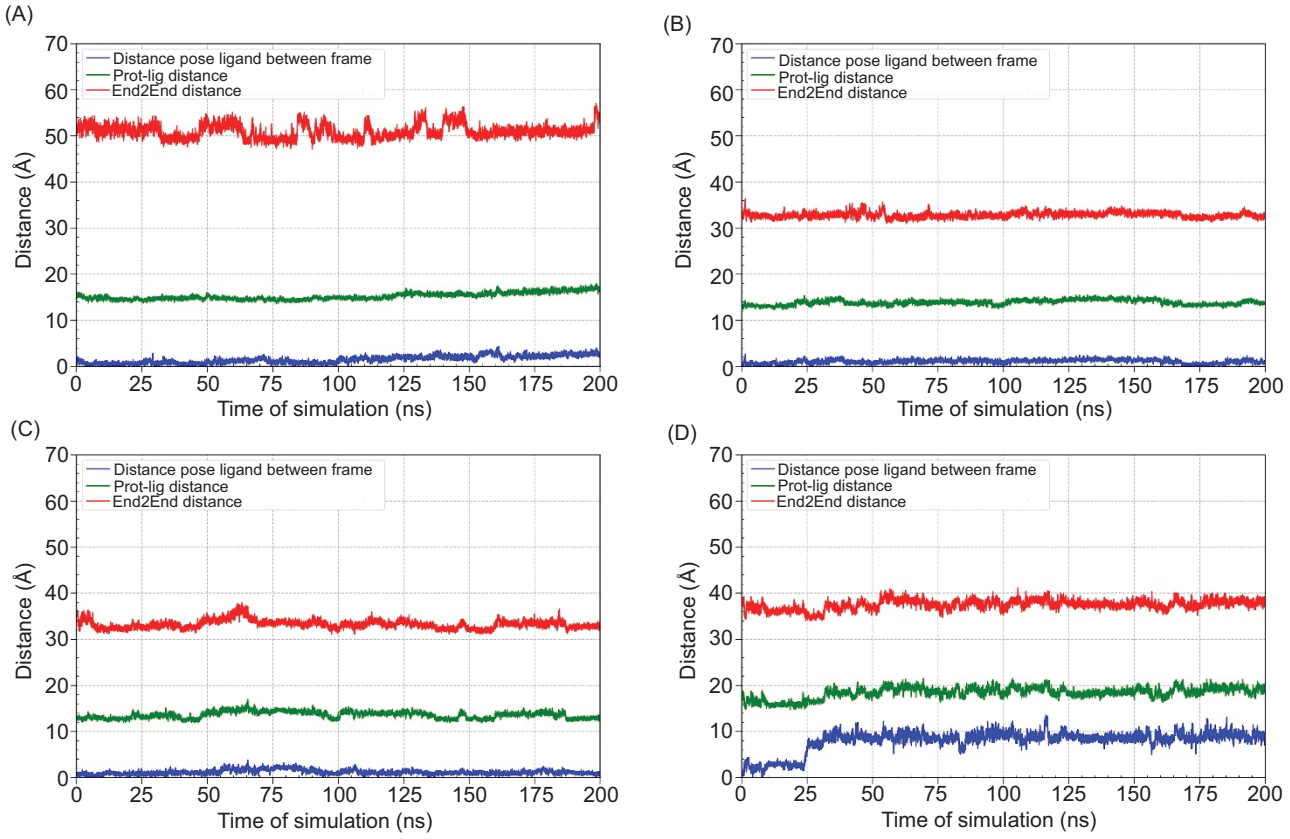

Figure 7 Distance analysis over 200 ns molecular dynamics simulations of the ligand-protein complexes. (A) MAOB-apigenin; (B) mGlu2-kaempferol; (C) mGlu2-dihydrokaempferol; (D) mGlu2-hydrangenol.

a pharmacological target for Parkinson's therapy (Elkamhawy et al., 2021; Kaur et al., 2023).

To complement this systems-level insight, molecular docking was conducted to predict ligand-target interactions for *Amaranthus*-derived compounds. We chose to conduct molecular docking first to explore the binding potential of all compounds without prematurely discarding compounds based on ADMET properties. After docking, we performed ADMET and bioactivity assessments. Finally, MD simulations were conducted to evaluate the stability and binding affinity of the ligand-protein complexes.

Docking identified apigenin, dihydrokaempferol, hydrangenol, and kaempferol as promising candidates, with reference ligands used to validate the method. Apigenin was identified as a strong MAOB inhibitor, likely due to its chromone-based structure that favors selective and stable hydrogen bonding (Mateev et al., 2023). Meanwhile, kaempferol, dihydrokaempferol, and hydrangenol were predicted to act on mGlu2 receptors, although lacking the typical orthosteric features of amino and carboxyl groups (Schoepp et al., 1999). Their structures, rich in hydroxyl and lactone moieties, suggest potential activity as positive allosteric modulators rather than direct agonists (Sheffler et al., 2011). Experimental validation is needed to confirm the stability and biological relevance of these predicted interactions.

ADMET predictions further evaluated these candidates, confirming that all four ligands met essential criteria for oral bioavailability, permeability, and blood-brain barrier penetration. Notably, apigenin exhibited a safer and more favorable pharmacokinetic profile, while dihydrokaempferol was highlighted for its strong predicted bioactivity, particularly as an antioxidant and anti-inflammatory agent. Hydrangenol's favorable BBB penetration was counterbalanced by its potential toxicity. Kaempferol also displayed acceptable absorption but a comparatively weaker safety and bioactivity profile.

To validate docking results under dynamic conditions, MD simulations were conducted over a 200 ns timescale to evaluate the stability of ligand-protein complexes. Binding free energies were estimated using the MM/GBSA method, an efficient end-state approach that calculates binding affinity from MD snapshots by analyzing intermolecular interactions. Solvent effects were incorporated via the generalized Born model, with nonelectrostatic contributions derived from solvent-accessible surface area (Taylor and Ho, 2023). RMSD

analyses were performed for proteins, ligands, and complexes. Protein RMSD values reflect conformational stability, whereas ligand RMSD indicates the stability of ligand binding within the active site. Lower RMSD values correspond to more stable systems (Sharma et al., 2022).

Among the ligands, dihydrokaempferol showed the most favorable binding free energy (ΔG_{total} = –29.803 kcal/mol), suggesting high thermodynamic affinity. However, its high solvation penalty (ΔG_{solv} = 29.963 kcal/mol) implies significant desolvation costs, aligned with RMSD fluctuations observed between 75 ns and 150 ns. Hydrangenol, though slightly weaker in binding affinity (ΔG_{total} = –25.415 kcal/mol), demonstrated the most consistent interaction, with stable RMSD and minimal energy fluctuations, indicating strong persistence within the binding pocket. Apigenin also exhibited favorable binding (ΔG_{total} = –27.675 kcal/mol), supported by stable nonpolar solvation and van der Waals contributions, despite minor structural adjustments later in the simulation. In contrast, kaempferol had the weakest binding (ΔG_{total} = –18.852 kcal/mol) and highest structural deviation, suggesting an unstable complex.

Based on the combined evaluation of docking, ADMET, bioactivity, and MD, dihydrokaempferol emerged as the most promising neuroprotective candidate due to its strong binding affinity, high bioactivity, and interaction with mGlu2, a key hub in the neuroprotective network. However, this strength is slightly limited by its less favorable pharmacokinetic profile and binding fluctuation. In contrast, apigenin demonstrated better pharmacokinetics and safety but targeted MAOB, a less central protein in the network. Overall, dihydrokaempferol offers the best neuroprotective potential, though further optimization is needed to address its pharmacokinetic limitations.

5. CONCLUSIONS

This study identifies D2, mGlu2, 5HT1A, GABAb, mGlu3, SERT, CB1, MORs, and MAOB as key protein targets involved in the neuroprotective effects. Molecular docking highlights apigenin as a potential MAOB inhibitor, whereas dihydrokaempferol, hydrangenol, and kaempferol show strong interactions with mGlu2. Among these, dihydrokaempferol emerges as the most promising neuroprotective candidate based on its strong binding affinity, high predicted bioactivity, and stable interactions in MD simulations despite pharmacokinetic limitations that warrant further optimization.

These findings lay the groundwork for further investigation of *Amaranthus*-derived compounds as potential adjunctive therapies for neurodegenerative disorders. Nevertheless, experimental validation is required to confirm the stability and biological relevance of these interactions. Future studies should include in vitro assays such as enzyme inhibition or neuroprotection assays using neuronal cell lines to verify the predicted interactions and biological activities. In addition, in vivo studies using animal models of neurodegenerative or mood disorders could be conducted to assess the pharmacodynamic and pharmacokinetic properties of the most promising compounds. These experimental validations will be essential to confirm the therapeutic potential and safety profiles of the identified ligands and to support their development as neuroprotective agents.

ACKNOWLEDGMENT

This article is part of the Masters Education to Doctorate for Excellence Undergraduate (Pendidikan Magister menuju Doktor untuk Sarjana Unggul [PMDSU]) research. In addition to the funding, the authors would like to thank Directorate General of Higher Education, Research, and Technology, Ministry of Education, Culture, Research, and Technology for their support throughout the project through PMDSU scholarship program.

FUNDING

This article was funded by the Directorate General of Higher Education, Research, and Technology, Ministry of Education, Culture, Research, and Technology for their financial support throughout the project, in accordance with the 2024 Research Program Implementation Contract Number 027/E5/PG.02.00. PL/2024, dated 11 June 2024.

CONFLICTS OF INTEREST

The authors declare no conflicts of interest.

ORCID

Mega Sonia Pertiwi	0009-0006-8051-4563
Irmanida Batubara	0000-0001-8201-7807
Rizka Fatriani	0000-0002-1739-8698
Setyanto Tri Wahyudi	0000-0003-0007-1186
Wisnu Ananta Kusuma	0000-0002-3682-244X
Trivadila Trivadila	0000-0003-0939-4635
Bambang Pontjo Priosoeryanto	0000-0001-5942-7402

AUTHORS CONTRIBUTIONS

Screening and docking, writing—original draft, final approval of the version to be submitted: M.S.P.; Conceptualisation and design of the study, validation, writing, review & editing, final approval of the version to be submitted: I.B.; Protein-protein network analysing, writing—original draft, final approval of the version to be submitted: R.F.; Molecular dynamics simulation, writing—original draft, final approval of the version to be submitted: S.T.W.; Validation, writing—review & editing, final approval of the version to be submitted: W.A.K.; Calidation, writing, review & editing, final approval of the version to be submitted: T.; Validation, writing, review & editing, final approval of the version to be submitted: B.P.P.

REFERENCES

Albert, P.R., 2020. Orphans to the rescue: Orphan G-protein coupled receptors as new antidepressant targets. Journal of Psychiatry and Neuroscience. 45, 301–303. https://doi.org/10.1503/jpn.200149

Anjum, R., Raza, C., Faheem, M., Ullah, A., Chaudhry, M., 2024. Neuroprotective potential of Mentha piperita extract prevents motor dysfunctions in mouse model of Parkinson's disease through anti-oxidant capacities. Public Library of Science One. 19, 1–18. https://doi.org/10.1371/journal.pone.0302102

Awaluddin, F., Batubara, I., Wahyudi, S.T., 2021. Molecular dynamics simulation of bioactive compounds against six protein target of Sars-Cov-2 as Covid-19 antivirus candidates. Jurnal Kimia Valensi. 7, 178–187. https://doi.org/10.15408/jkv.v7i2.21634

Beppe, G.J., Rebe, R.N., Maitemwa, M.-I., Folefack, A.I., Barga, B.P., Allah-doum, N.G., Dongmo, A.B., 2024. Neuroprotective impact of Ximenia americana aqueous bark extract on diazepam-induced memory impairment in mice via its antioxidant potential. Notulae Scientia Biologicae. 16, 1–15. https://doi.org/10.15835/nsb16111713

Bi, D., Wen, L., Wu, Z., Shen, Y., 2020. GABAergic dysfunction in excitatory and inhibitory (E/I) imbalance drives the pathogenesis of Alzheimer's disease. Alzheimer's and Dementia. 1–18. https://doi.org/10.1002/alz.12088

Bledsoe, R.K., Madauss, K.P., Holt, J.A., Apolito, C.J., Lambert, M.H., Pearce, K.H., Stanley, T.B., Stewart, E.L., Trump, R.P., Willson, T.H., Williams, S.P., 2005. A ligand-mediated hydrogen bond network required for the activation of the mineralocorticoid receptor. The Journal of Biological Chemistry. 280, 31283–31293. https://doi.org/10.1074/jbc.M504098200

Cahya, H.D., Nurlela, N., Tohir, D., Batubara, I., Asoka, S.F., Yamauchi, K., 2024. Potential of active compounds in broadleaf mahogany (Swietenia macrophylla) seeds against breast cancer cells based on in silico study. Jurnal Jamu Indonesia 9, 41–51. https://doi.org/10.29244/jji.v9i1.296

Chen, C., Zhou, X., He, J., Xie, Z., Xia, S., Lu, G., 2019. The roles of GABA in ischemia-reperfusion injury in the central nervous system and peripheral organs. Oxidative Medicine and Cellular Longevity. 2019, 1–19. https://doi.org/10.1155/2019/4028394

Chin, C.H., Chen, S.H., Wu, H.H., Ho, C.W., Ko, M.T., Lin, C.Y., 2014. cytoHubba: Identifying hub objects and sub-networks from complex interactome. BioMed Central Systems Biology. 8, 1–7. https://doi.org/10.1186/1752-0509-8-S4-S11/TABLES/4

Consortium, The Uniprot, 2023. UniProt: the universal protein knowledgebase in 2023. Nucleic Acids Res. 51, D523–D531. https://doi.org/10.1093/nar/gkac1052

Demos-Davies, K., Lawrence, J., Coffey, J., Morgan, A., Ferreira, C., Hoeppner, L.H., Seelig, D., 2024. Longitudinal neuropathological consequences of extracranial radiation therapy in mice. International Journal of Molecular Sciences. 25. https://doi.org/10.3390/ijms25115731

Elek, M., Djokovic, N., Frank, A., Oljacic, S., Zivkovic, A., Nikolic, K., Stark, H., 2021. Synthesis, in silico, and in vitro studies of novel dopamine D2 and D3 receptor ligands. Archiv der Pharmazie – Chemistry in Life Sciences. 354. https://doi.org/10.1002/ardp.202000486

Elkamhawy, A., Woo, J., Gouda, N.A., Kim, J., Nada, H., Roh, E.J., Park, K.D., Cho, J., Lee, K., 2021. Melatonin analogues potently inhibit mao-b and protect pc12 cells against oxidative stress. Antioxidants. 10, 1–27. https://doi.org/10.3390/antiox10101604

Fang, S., Zhong, L., Wang, A. quan, Zhang, H., Yin, Z.S., 2021. Identification of regeneration and hub genes and pathways at different time points after spinal cord injury. Molecular Neurobiology. https://doi.org/10.1007/s12035-021-02289-x

Gargano, A., Beins, E., Zimmer, A., Bilkei-Gorzo, A., 2021. Lack of cannabinoid receptor type-1 leads to enhanced age-related neuronal loss in the locus coeruleus. International Journal of Molecular Sciences. 22, 1–16. https://doi.org/10.3390/ijms22010005

González-Fuentes, J., Selva, J., Moya, C., Castro-Vázquez, L., Lozano, M. V., Marcos, P., Plaza-Oliver, M., Rodríguez-Robledo, V., Santander-Ortega, M.J., Villaseca-González, N., Arroyo-Jimenez, M.M., 2018. Neuroprotective natural molecules, from food to brain. Frontiers in Neuroscience. 12, 1–8. https://doi.org/10.3389/fnins.2018.00721

Grewal, A., Sheokand, D., Chauhan, R., Saini, V., Kumar, A., 2024. Insights into amyloid precursor protein target through PPI network analysis. Bioinformation. 20, 140–145. https://doi.org/10.6026/973206300200140

Haase, J., Brown, E., 2015. Integrating the monoamine, neurotrophin and cytokine hypotheses of depression – A central role for the serotonin transporter? Pharmacology & Therapeutics. 147, 1–11. https://doi.org/10.1016/j.pharmthera.2014.10.002

Hashimoto, K., 2018. Essential role of Keap1-Nrf2 signaling in mood disorders: Overview and future perspective. Frontiers in Pharmacology. 9. https://doi.org/10.3389/fphar.2018.01182

Hollingsworth, S.A., Dror, R.O., 2018. Molecular dynamics simulation for all. Neuron. 99, 1129–1143. https://doi.org/10.1016/j.neuron.2018.08.011

Jaronczyk, M., Walory, J., 2022. Novel molecular targets of antidepressants. Molecules. 27. https://doi.org/10.3390/molecules27020533

Jelen, L.A., Stone, J.M., Young, A.H., Mehta, M.A., 2022. The opioid system in depression. Neurosci. Neuroscience and Biobehavioral Reviews. 140. https://doi.org/10.1016/j.neubiorev.2022.104800

Kaur, G., Goyal, D., Goyal, B., 2023. Computational modeling of MAO inhibitors as anti-Alzheimer agents. Neuromethods. 203, 325–353. https://doi.org/10.1007/978-1-0716-3311-3_11

Kosmopoulou, D., Lafara, M.P., Adamantidi, T., Ofrydopoulou, A., Grabrucker, A.M., Tsoupras, A., 2024. Neuroprotective benefits of Rosmarinus officinalis and its bioactives against Alzheimer's and Parkinson's diseases. Applied Sciences. 14. https://doi.org/10.3390/app14156417

Lalkovičová, M., Danielisová, V., 2016. Neuroprotection and antioxidants. Neural Regeneration Research. 11, 865–874. https://doi.org/10.4103/1673-5374.184447

Lv, Y., Zheng, Z., Liu, R., Guo, J., Zhang, C., Xie, Y., 2023. Monoamine oxidase B inhibitors based on natural privileged scaffolds: A review of systematically structural modification. International Journal of Biological Macromolecules. 251. https://doi.org/10.1016/j.ijbiomac.2023.126158

Malik, R., Kalra, S., Pooja, Singh, G., Meenu, Gahlot, V., Kajal, A., Rimpy, 2024. Antioxidative and neuroprotective potential of Acorus calamus linn. and Cordia dichotoma G. Forst. In Alzheimer's type dementia in rodent. Brain Research. 1822. https://doi.org/10.1016/j.brainres.2023.148616

Mateev, E., Georgieva, M., Mateeva, A., Zlatkov, A., Ahmad, S., Raza, K., Azevedo, V., Barh, D., 2023. Structure-based design of novel MAO-B inhibitors: A review. Molecules. 28. https://doi.org/10.3390/molecules28124814

Moazzem Hossen, S.M., Akramul Hoque Tanim, M., Shahadat Hossain, M., Ahmed Sami, S., Uddin Emon, N., 2021. Deciphering the CNS anti-depressant, antioxidant and cytotoxic profiling of methanol and aqueous extracts of Trametes versicolor and molecular interactions of its phenolic compounds. Saudi Journal of Biological Sciences. 28, 6375–6383. https://doi.org/10.1016/j.sjbs.2021.07.016

Ostrowska, K., Grzeszczuk, D., Głuch-Lutwin, M., Gryboś, A., Siwek, A., Leśniak, A., Sacharczuk, M., Trzaskowski, B., 2018. 5-HT1A and 5-HT2A receptors affinity, docking studies and pharmacological evaluation of a series of 8-acetyl-7-hydroxy-4-methylcoumarin derivatives. Bioorganic & Medicinal Chemistry. 26, 527–535. https://doi.org/10.1016/j.bmc.2017.12.016

Paggi, J.M., Pandit, A., Dror, R.O., 2024. The art and science of molecular docking. Annual Review of Biochemistry. 93, 389–410. https://doi.org/10.1146/annurev-biochem-030222-120000

Patel, S., Hillard, C.J., 2009. Role of endocannabinoid signaling in anxiety and depression. Current Topics in Behavioral Neurosciences. 1, 1–21. https://doi.org/10.1007/978-3-540-88955-7_14

Pertiwi, M.S., Batubara, I., Indariani, S., Murni, A., Wati, V.S., 2024. Potential indonesian plants as energy boosters. Reviews in Agricultural Science. 12, 401–420. https://doi.org/https://doi.org/10.7831/ras.12.0_403

Peter, K., Gandhi, P., 2017. Rediscovering the therapeutic potential of Amaranthus species: A review. Egyptian Journal of Basic and Applied Sciences. 4, 196–205. https://doi.org/10.1016/j.ejbas.2017.05.001

Qi, W., Jin, X., Guan, W., 2024. Purinergic P2X7 receptor as a potential therapeutic target in depression. Biochemical Pharmacology. 219. https://doi.org/10.1016/j.bcp.2023.115959

Rayasam, G.V., Tulasi, V.K., Sodhi, R., Davis, J.A., Ray, A., 2009. Glycogen synthase kinase 3: More than a namesake. British Journal of Pharmacology. 156, 885–898. https://doi.org/10.1111/j.1476-5381.2008.00085.x

Robati, R.M., Bandarian, F., Razi, F., Razzaghi, Z., Nejad, M.R., Rezaei, M., Arjmand, B., Mansouri, V., 2024. Rutin effects on human senescent stromal cells function: A network analysis study. Research Journal of Pharmacognosy. 11, 59–66. https://doi.org/10.22127/rjp.2024.463377.2506

Schoepp, D.D., Jane, D.E., Monn, J.A., 1999. Pharmacological agents acting at subtypes of metabotropic glutamate receptors. Neuropharmacology. 38, 1431–1476. https://doi.org/10.1016/S0028-3908(99)00092-1

Shamsi, A., Khan, M.S., Yadav, D.K., Shahwan, M., Furkan, M., Khan, R.H., 2024. Structure-based drug-development study against fibroblast growth factor receptor 2: Molecular docking and molecular dynamics simulation approaches. Scientific Reports. 14, 1–13. https://doi.org/10.1038/s41598-024-69850-1

Shannon, P., Markiel, A., Ozier, O., Baliga, N.S., Wang, J.T., Ramage, D., Amin, N., Schwikowski, B., Ideker, T., 2003. Cytoscape: A software environment for integrated models of biomolecular interaction networks. Genome Research. 13, 2498–2504. https://doi.org/10.1101/gr.1239303

Sharma, A., Vora, J., Patel, D., Sinha, S., Jha, P.C., Shrivastava, N., 2022. Identification of natural inhibitors against prime targets of SARS-CoV-2 using molecular docking, molecular dynamics simulation and MM-PBSA approaches. The Journal of Biomolecular Structure and Dynamics. https://doi.org/10.1080/07391102.2020.1846624

Sheffler, D.J., Pinkerton, A.B., Dahl, R., Markou, A., Cosford, N.D.P., 2011. Recent progress in the synthesis and characterization of group II metabotropic glutamate receptor allosteric modulators. American Chemical Society Chemical Neuroscience. 2, 382–393. https://doi.org/10.1021/cn200008d

Silva, R.F.M., Pogačnik, L., 2020. Polyphenols from food and natural products: Neuroprotection and safety. Antioxidants. 9, 1–13. https://doi.org/10.3390/antiox9010061

Srivastava, A., Das, B., Yao, A.Y., Yan, R., 2020. Metabotropic glutamate receptors in Alzheimer's disease synaptic dysfunction: Therapeutic opportunities and hope for the future. Journal of Alzheimer's Disease. 78, 1345–1361. https://doi.org/10.3233/JAD-201146

Sung, Y.K., Kyou, C.C., Min, S.C., Myoung, H.K., Sa, Y.K., Na, Y.S., Jong, E.L., Byung, K.J., Lee, B.H., Baik, J.H., 2006. The dopamine D2 receptor regulates the development of dopaminergic neurons via extracellular signal-regulated kinase and Nurr1 activation. The Journal of Neuroscience. 26, 4567–4576. https://doi.org/10.1523/JNEUROSCI.5236-05.2006

Szklarczyk, D., Kirsch, R., Koutrouli, M., Nastou, K., Mehryary, F., Hachilif, R., Gable, A.L., Fang, T., Doncheva, N.T., Pyysalo, S., Bork, P., Jensen, L.J., von Mering, C., 2022. The STRING database in 2023: Protein–protein association networks and functional enrichment analyses for any sequenced genome of interest. Nucleic Acids Research. 51, D638–D646. https://doi.org/10.1093/nar/gkac1000

Taylor, M., Ho, J., 2023. MM/GBSA prediction of relative binding affinities of carbonic anhydrase inhibitors: Effect of atomic charges and comparison with Autodock4Zn. Journal of Computer-Aided Molecular Design. 37, 167–182. https://doi.org/10.1007/s10822-023-00499-0

Wang, Y., Wang, Y.X., Liu, T., Law, P.Y., Loh, H.H., Qiu, Y., Chen, H.Z., 2015. μ-Opioid receptor attenuates Aβ oligomers-induced neurotoxicity through mTOR signaling. Cognitive Neuroscience Society Neuroscience & Therapeutics. 21, 8–14. https://doi.org/10.1111/cns.12316

Yugandhar, K., Gromiha, M.M., 2016. Analysis of protein-protein interaction networks based on binding affinity. Current Protein and Peptide Science. 17, 72–81. https://doi.org/10.2174/1389203716666150923105907

Zhou, H.Q., Zhuang, L.J., Bao, H.Q., Li, S.J., Dai, F.Y., Wang, P., Li, Q., Yin, D.M., 2022. Olfactory regulation by dopamine and DRD2 receptor in the nose. Proceedings of the National Academy of Sciences of the United States of America. 119, 1–10. https://doi.org/10.1073/pnas.2118570119